P5.17 ICE NUCLEATION EXPERIMENTS AT SIMULATED CLOUD CONDITIONS

Ottmar Möhler*, Simone Schaefers, Olaf Stetzer, and Ulrich Schurath
Institute of Meteorology and Climate Research, Forschungszentrum Karlsruhe, Germany

Alexander Mangold and Martina Krämer
ICG-1, Forschungszentrum Jülich, Germany

1. INTRODUCTION

Ice nucleation (IN) plays a key role in the formation of cirrus clouds or the initiation of precipitation in lower tropospheric clouds. It can occur either by homogeneous freezing of pure water and solution droplets below about –35°C (Koop et al., 2000: Pruppacher and Klett, 1997), or be heterogeneously induced by so-called ice nuclei (Vali, 1996). A quantitative description of the ice nucleation processes is crucial for a better understanding of formation, life cycles, and optical properties of clouds.

The large coolable and evacuable aerosol chamber facility AIDA (aerosol interaction and dynamics in the atmosphere) is used as a cloud chamber to study processes of ice formation at simulated tropospheric cloud conditions. A wide range of temperature, pressure, cooling rate and relative humidity can be established during ice activation experiments covering conditions throughout the troposphere and lower stratosphere under which water clouds, mixed clouds, cirrus clouds, and even Polar Stratospheric Clouds (PSC) are formed (Nink et al., 2000: Zink et al., 2002). This paper briefly describes major technical components, experimental methods, and results of heterogeneous IN experiments with soot aerosol.

2. EXPERIMENTAL

2.1. AIDA Aerosol Chamber Facility

Figure 1 depicts a scheme of major technical parts of the AIDA facility together with instrumentation used for IN expansion experiments. The cylindrical aerosol vessel with a volume of 84 m^3 is located inside a thermal insulating box. The interior of the box can homogeneously be cooled to any temperatures cooled to any temperatures between 183 K and room temperature. At static T,p-conditions, the relative humidity with respect to ice (RHi) inside the aerosol vessel can be controlled from close to 100% to below 1 %. To achieve RHi close to 100%, the aerosol vessel is filled with humidified synthetic air at higher temperatures and thereafter slowly cooled to a temperature markedly below the frost point temperature. The excess water is deposited on the vessel walls forming a thin ice coating.

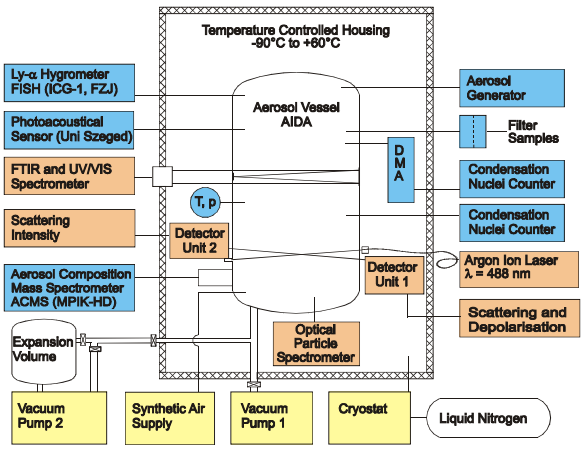

Figure 1: Schematic of the AIDA aerosol and cloud chamber facility.

In preparation of each IN experiment at ice-coated wall conditions, the aerosol vessel is pumped off to a pressure below 0.1 hPa and refilled with dry synthetic air to a pressure of 1000 hPa. Adding of humidified air to the cold aerosol vessel would cause the formation of an undesired background of ice nuclei. After filling is completed the ice coating provides almost ice saturated conditions inside the aerosol vessel within about 30 min.

Thereafter, soot aerosol particles are added at number concentrations between 1000 and 3000 cm^{-3}. The soot aerosol is taken from a graphite sparc generator (GfG1000, Palas). The soot particles are fractal like aggregates with mobility equivalent diameters around 100 nm

* *Corresponding author address:* Ottmar Möhler, Institute of Meteorology and Climate Research, Forschungszentrum Karlsruhe, 76021 Karlsruhe, Germany; e.mail: Ottmar.Moehler@imk.fzk.de

and composed of primary particles with diameters of about 4 nm.

2.2. Experimental Method of Ice Activation

All heterogeneous IN experiments discussed in this paper are started at constant pressure of about 1000 hPa and ice saturation ratio close to 1 (RHi close to 100%). Ice supersaturation needed for IN of soot particles is achieved by volume expansion due to controlled pumping using two large vacuum pumps at different pumping speeds. Depending on starting temperature and pumping speed, the regime between ice and water saturation is passed within a few minutes at cooling rates up to 200 K/h.

Figure 2 depicts time series of pressure, mean gas temperature, ice saturation ratio, and depolarisation (see below) during a fast expansion started at 980 hPa and 234 K. The expansion to a final pressure of 800 hPa lasted about 3.5 min. The highest cooling rates are only achieved within the first few minutes. Hereafter, a steady state is achieved between further adiabatic cooling and heat transfer from the 2 cm thick aluminum walls remaining at constant temperature during expansion due to their high heat capacity. After pumping is stopped the gas temperature increases and approaches wall temperature on a time scale of about five minutes. Volume expansion into an evacuated vessel of 4 m^3 volume can additionally be used to sharply increase the ice saturation ratio by about 0.2 within a few seconds.

Evaporation of ice phases is forced by controlled adiabatic heating of the chamber gas during refilling the chamber with dry synthetic air. Thereafter, the next IN activation cycle is started with the same aerosol that was only diluted by about 20% after pumping from about 1000 to 800 hPa.

Water vapour mixing ratio and partial pressure are measured with three independent instruments, (1) the FISH Lyman-α hygrometer of Forschungszentrum Jülich (Zöger et al., 1999), (2) the prototype of a novel photoacoustic water vapour sensor (PAS) developed and operated by the University of Szeged, Hungary (Szakáll et al., 2001), and (3) a commercial chilled mirror hygrometer from General Eastern. All instruments are operated outside the chamber using the same heated sampling tube. Therefore, the hygrometers measure the total water (gas and ice phase). Until the onset of ice particle formation, these data can be used to calculate the ice saturation ratio. The saturation vapour pressure is calculated from the mean gas temperature using the parameterisation given by (Marti and Mauersberger, 1993).

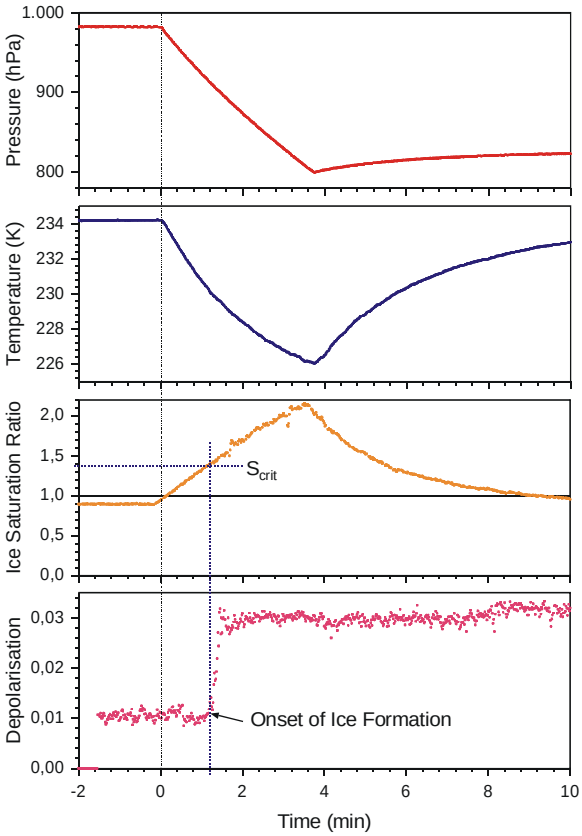

Figure 2: Time series of pressure, mean gas temperature, ice saturation ratio, and depolarisation ratio for a typical expansion experiment.

2.3. Detection of Ice Formation

The onset of ice formation during IN expansion experiments is detected by measuring the depolarisation of scattered laser light with high sensitivity and time resolution. An Argon-Ion laser beam (99% polarized radiation at 488 nm) is conducted into the chamber via an optical fiber which preserves the plane of polarization (Figure 1). The laser beam and the aperture of the detection optics overlap in the middle of the chamber at a distance of 2 m from the walls, providing about 2 cm^3 of scattering volume. The scattered light is split into the parallel and the perpendicular components by a Glan-Taylor prism and then detected by two independent photomultipliers. Detector optics are mounted at scattering angles of 176° and 4°. This setup provides information on the volume, size, and

phase of the scattering aerosol. The data set allows for a precise determination of the onset of ice formation and the formation and growth of liquid and solid aerosol particles.

After onset of ice formation the calculated ice saturation ratio is overestimated by the ice water content that rapidly increases due to uptake of water on ice particles. Number concentration and optical sizes of ice particles are measured with an optical particle spectrometer (PCS2000, Palas) operated below the aerosol vessel (c.f. figure 1). Residence times in the cold vertical sampling tube are short enough to minimise evaporation of ice particles. Information about the ice phase is also obtained from *in situ* multi-path FTIR extinction spectroscopy. The dynamic growth and evaporation of ice particles is investigated by comparing the measured data with respective process models. This work is in progress and is not discussed in this paper.

The size distribution of the soot aerosol particles is measured with a differential mobility analyser (DMA). The total aerosol number concentration is measured with a condensation nuclei counter (CNC). The DMA and CNC have been modified for operation at sampling pressures between 100 and 1000 hPa.

3. RESULTS

The heterogeneous IN of soot aerosol was investigated at temperatures between 192 and 250 K (Figure 3). The critical ice saturation ratio needed for IN, S_{IN}, was measured as outlined in Figure 2. At temperatures above 235 K, IN of soot particles only occurs close to or slightly above water saturation (solid blue line in Figure 3). Liquid water seems to condense on the soot particles before ice activation occurs (immersion freezing).

At lower temperatures ice is formed significantly below the liquid water saturation threshold and also below the threshold for homogeneous freezing nucleation of supercooled liquid solution droplets indicated by the dashed blue line (Koop et al., 2000). Decreasing S_{IN} with decreasing temperatures was also found by DeMott (DeMott et al., 1999) who measured IN of redispersed Degussa soot at temperatures between 213 and 233 K. In that study, significant decrease of the S_{IN} below the values of homogeneous IN was only measured for soot treated with 'multilayer' sulphuric acid coating. At 213 K, S_{IN} measured for multi-layer sulphuric acid Degussa soot by DeMott et al. (1999) agrees with the AIDA data measured for untreated sparc generator soot. The first AIDA measurements below 213 K indicate a slight increase of S_{IN}. This trend has to be confirmed by further data currently analysed.

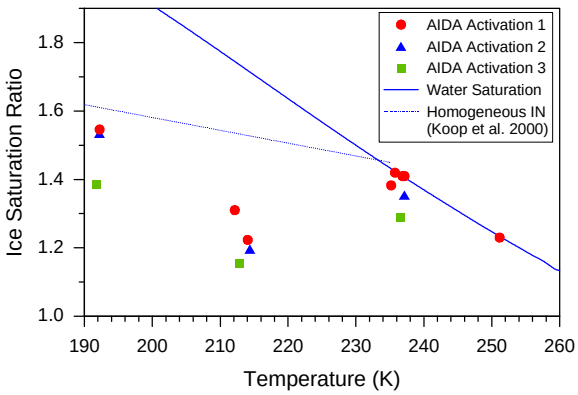

Figure 3: Measured ice saturation ratio for onset of ice formation in soot aerosol as function of temperature and number of subsequent activations.

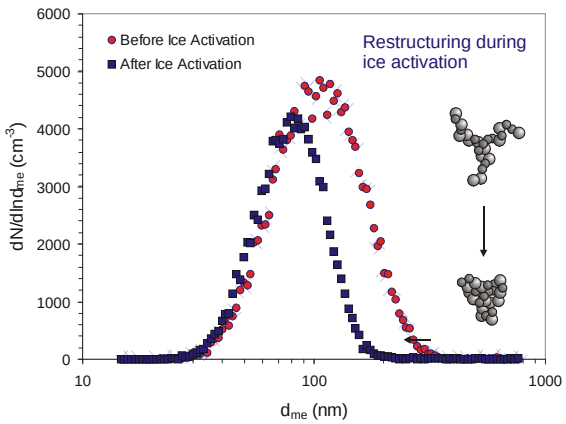

Figure 4: Aerosol number size distribution measured with a mobility analyser before and after ice activation.

At 192, 213, and 235 K, S_{IN} was found to significantly decrease in subsequent ice activation and evaporation cycles of the same soot aerosol (c.f. different symbols in Figure 3). This decrease may be caused by 'ageing' effects, e.g. changing agglomerate and surface structure, during the ice activation process. During the first ice activation of fresh soot particles, significant shrinking can be derived from size distribution measurements with the mobility analyser (Figure 4). The decrease of mean mobility equivalent diameter can only be explained by the indicated restructuring process.

4. SUMMARY AND CONCLUSIONS

In the AIDA experimental facility, ice activation experiments are performed by simulating cycles of ice and water super- and subsaturations, using the method of expansion-cooling. Relative humidity can dynamically be increased in a controlled manner from ice saturation to values above water saturation within several minutes. The critical ice saturation ratio for the onset of IN, S_{IN}, was measured for untreated soot aerosol at temperatures between 192 and 250 K. At temperatures above 235 K, IN seems to occur only after liquid activation of the soot particles, whereas at lower temperatures deposition freezing was measured at ice saturation ratios between 1.2 at 213 K and 1.5 at 192 K, significantly below water saturation and below homogeneous IN of solution droplets.

One of the major advantages of AIDA ice nucleation experiments is the fact that only a minor fraction of the aerosol is lost during expansion cycles. Therefore, ageing effects on IN of aerosols can be investigated in repeated activation and evaporation cycles. First results show a significant decrease of S_{IN} for untreated soot in three subsequent activation cycles. Further data analysis will focus on the fraction of activated soot particles depending on e.g. the cooling rate. The dynamic growth and evaporation process of ice particles will also be analysed.

5. REFERENCES

DeMott, P. J., Y. Chen, S. M. Kreidenweis, D. C. Rogers, and D. E. Sherman, 1999: Ice formation by black carbon particles. *Geophysical Research Letters*, **26,** 2429-2432.

Koop, T., B. Luo, A. Tsias, and T. Peter, 2000: Water activity as the determinant for homogeneous ice nucleation in aqueous solutions. *Nature*, **406,** 611-614.

Marti, J. and K. Mauersberger, 1993: A survey and new measurements of ice vapor pressure at temperatures between 170 and 250 K. *Geophysical Research Letters*, **20,** 363-366.

Nink, A., H. Saathoff, M. Schnaiter, and O. Möhler, 2000: Laboratory investigation of the impact if aircraft particulate emissions on cirrus cloud formation. *European workshop on aviation, aerosols, contrails, and cirrus clouds (A2C3)*, Seeheim, EUR, 149-153.

Pruppacher, H. R. and J. D. Klett, 1997: *Microphysics of clouds and precipitation*. Kluwer Academic Publishers.

Szakáll, M., Z. Bozóki, M. Krämer, N. Spelten, O. Möhler, and U. Schurath, 2001: Evaluation of a photoacoustic detector for water vapor measurements under simulated tropospheric/lower stratospheric conditions. *Environmental Science and Technology*, **35,** 4881-4885.

Vali, G., 1996: Ice nucleation - a review. *14th. International Conference on Nucleation and Atmospheric Aerosols*, Helsinki, Finland, Pergamon Press.

Zink, P., D. A. Knopf, J. Schreiner, K. Mauersberger, O. Möhler, H. Saathoff, M. Seifert, R. Tiede, and U. Schurath, 2002: Cryo-chamber simulation of stratospheric H_2SO_4/H_2O particles: composition analysis and model comparison. *Geophysical Research Letters*, **(in press)**.

Zöger, M., A. Afchine, N. Eicke, M.-T. Gerhards, E. Klein, D. S. McKenna, U. Mörschel, U. Schmidt, V. Tan, F. Tuitjer, T. Woyke, and C. Schiller, 1999: Fast in situ stratospheric hygrometers: A new family of balloon-borne and airborne Lyman α photofragment fluorescence hygrometers. *Journal of Geophysical Research*, **104,** 1807-1816.